A Model for Molecular Weights in Vinyl Acetate Emulsion Polymerization

The continuous stirred tank emulsion polymerization of vinyl acetate has shown oscillatory behavior in conversion, particle size, molecular weight, and polydispersity during polymerization. The kinetics in vinyl acetate emulsion polymerization are especially complex because of chain transfer to polymer and monomer and the terminal double bond reaction. A nonsteady-state model to predict the average molecular weights is developed for this polymerization system. Improved results are achieved by inclusion of the effects of polymer chain initiation and termination by absorbed radicals. It is found that the observed oscillations are closely related to the radical diffusion and desorption rates that are involved in a heterogeneous initiation mechanism. The molecular weights and polydispersities are successfully predicted by the model. The nature of the oscillations in these properties is examined.

Chan H. Lee, Richard G. Mallinson
School of Chemical Engineering
and Materials Science
University of Oklahoma
Norman, OK 73019

Introduction

Continuous emulsion polymerization is an important industrial process because of the high output and consistent product quality achieved. One of the most complicated phenomena that has been observed in continuous emulsion polymerization is oscillatory behavior. That is, oscillations about a steady state of the number of polymer particles, average particle sizes, and polymer molecular weights. Since Omi et al.'s (1969) theoretical attempts to explain these property oscillations, much experimental and theoretical effort has been made to model this continuous emulsion polymerization system (Min and Ray, 1974; Dickinson, 1976; Greene et al., 1976; Kirillov and Ray, 1978; Kiparissides, 1978; Kiparissides et al., 1979, 1980a,b; Rawlings 1985; Rawlings and Ray 1987). Both the models of Kiparissides et al. and Rawlings and Ray have shown good agreement with experimental data for conversion. A basic difference between these models is the calculation of the average number of radicals per particle. Kiparissides et al. use a simplified formula suggested by Ugelstad and Hansen (1976) for vinyl acetate, while Rawlings (1985) uses the general relation for the average number of radicals per particle of Stockmayer (1957) and O'Toole (1965). The model of Kiparissides et al. involves integro-differential equations that were transformed to ordinary differential equation form for easier implementation by Chiang and Thompson (1979). These modeling studies were concerned with conversion and average particle size. In modeling the molecular weight, Min and Ray (1974) presented a generalized framework that is the most general and extensive development. However, actual simulations to predict unsteady-state molecular weights have not been attempted.

The reaction mechanism in vinyl acetate emulsion polymerization is complex because it includes chain transfer to monomer and polymer, the terminal double bond reaction, and a diffusion-controlled initiation mechanism. Detailed investigations of the kinetics of vinyl acetate polymerization have been published by Graessley and coworkers (Graessley et al., 1969; Saito et al., 1969; Nagasubramanian and Graessley, 1970). That work was mainly associated with bulk and solution polymerization of vinyl acetate at low initiation rates. Later, Hamielec and coworkers (Friis and Hamielec, 1975; Pollock et al., 1982) proposed a modification of Graessley's model by neglecting initiation and termination rates. This simplification may not be appropriate at low conversions or high initiation rates. Taylor and Reichert (1985) later simulated this system by considering initiation and termination steps in a molecular weight model, but considered only solution polymerization. In contrast to bulk and solution polymerizations, emulsion polymerization undergoes heterogeneous initiation and termination mechanisms, i.e., initiation and termination by radical absorption from the water phase into the polymer particles and micelles. In this paper, a detailed nonsteady-state molecular weight model is derived which accounts for the transient molecular weight behavior. A comparison is then made between the model results and new experimental data for this system.

Correspondence concerning this paper should be addressed to R. G. Mallinson.

Reaction Mechanism

Many complex phenomena are involved in the emulsion polymerization of vinyl acetate. In order to properly account for these effects, the basic assumptions for the mechanistic model must first be mentioned. A kinetic mechanism for vinyl acetate emulsion polymerization includes the usual reaction steps: chain initiation, propagation, branching, and termination. The physical mechanisms involved in this model formulation are four:

First, it is assumed that the initiator decomposes into free radicals in the aqueous phase and these primary radicals enter newly generated micelles and polymer particles directly without further propagation, and that the major polymerization locus is in the particles (Harkins, 1945, 1946, 1947; Smith and Ewart, 1948). Actually, some of the initiator radicals may propagate with solubilized monomer molecules before entering the particles and micelles. However, it is not a significant effect for calculations of the average molecular weight as long as the chain length of the propagated radicals in the water phase is not too long. For simplification, direct absorption was introduced as a basis.

Second, the growing polymer particles cannot accommodate more than one radical. This assumption means that there is immediate termination when a radical enters a particle already containing a radical, instead of starting a new chain (Ugelstad and Hansen, 1976; Hansen and Ugelstad, 1978, 1979).

Third, only monomeric radicals may desorb from the particles. Long-chain radicals may not desorb because of high viscosity in the particles and low solubility in the aqueous phase (Nomura and Harada, 1981; Nomura, 1982).

Finally, termination occurs only by primary and monomeric radicals from the aqueous phase. The major termination mode is disproportionation.

From these assumptions we may now formulate the mechanistic steps by including the standard polymerization reactions for vinyl acetate monomer.

Initiation

Chain initiation may proceed by following one of several mechanisms. As we have stated, the propagating polymer chains may be generated by entry of water phase radicals, which consist of primary radicals—which are initiator fragments produced from initiator decomposition—and monomeric radicals, which have desorbed from particles into micelles and polymer particles that have no propagating radicals.

The absorbed *primary* radicals produce monomeric radicals by reacting with monomer molecules.

$$[R\cdot]_p + [M_p] \xrightarrow{K_i} [P_o^*]$$

The lifetime of the absorbed primary radicals is very short and these radicals are not desorbed due to fast propagation. Therefore, the rate of this step may be approximated by using a stationary-state hypothesis for the continuous reactor:

$$K_i[R\cdot]_p[M_p] = K_1[R\cdot]_w[m_s] + K_2[R\cdot]_w[N_o] \qquad (1)$$

where the first and second terms on the righthand side are rates for micelles and dead polymer particles, respectively. Monomeric radicals in the particles are also produced by direct absorption of monomeric radicals from the water phase into micelles and dead polymer particles.

$$[M_1\cdot] + [m_s] \xrightarrow{K_1} [P_o^*]$$

$$[M_1\cdot] + [N_o] \xrightarrow{K_2} [P_o^*]$$

The major chemical structure of the monomeric radicals is $CH_2{=}\dot{C}{-}OCOCH_3$. Monomeric radicals in the water phase are produced primarily by desorption of monomeric radicals from particles. Constant K_1 was calculated from Fick's first law, and for K_2 the Smith-Ewart second idealized situation was considered.

Propagation

The monomeric radicals, once within particles and micelles, quickly propagate. It is assumed that the rate constant is independent of the polymer chain length and constant throughout the polymerization.

$$[P_j^*] + [M_p] \xrightarrow{K_p} [P_{j+1}^*]$$

Chain transfer

One of the chain length controlling reactions that occurs in this polymerization is chain transfer. The transfer agents may be adsorbed surfactant molecules, impurities contained in surfactant, monomer molecules, and dead polymer chains. Only two possibilities are considered here for the polymerization of vinyl acetate. These are transfer to monomer and transfer to dead polymer chains.

$$[P_j^*] + [M_p] \xrightarrow{K_{mf}} [P_j] + [P_o^*]$$

$$[P_j^*] + [P_m] \xrightarrow{K_{trp}} [P_j] + [P_m^*]$$

Terminal double bond reaction

The terminal double bond reaction is a type of multiple propagation. For vinyl acetate this reaction was first recognized by Graessley et al. (1969). This reaction leads to a dramatic increase in molecular weight. To include this effect it may be necessary to distinguish between two types of dead polymer chains: one with a terminal double bond and the other without this bond. For this system, a large fraction of the dead polymer chains has terminal double bonds due to transfer to monomer and the disproportionation mode of termination. We do not differentiate between them to reduce complexities. Neglecting this difference may tend to overemphasize this phenomenon.

$$[P_j^*] + [P_m] \xrightarrow{K_{pp}} [P_{j+m}^*]$$

Termination

During the polymerization, there exist entangled dead polymer chains and solubilized monomer in the core of the particles. The active ends of living polymer chains are probably located near the adsorbed surfactant head groups and the first few carbon atoms of their hydrophobic tails, called the palisade layer. This is due to the polarity of the propagating radical and the continuous diffusion of monomer from the water phase. The dif-

fusing vinyl acetate monomer may also tend to locate in the palisade layer due to its relatively hydrophilic nature. The exact location at which solubilization may occur varies with dipole–dipole attractions or H-bonding (Rosen, 1978). The propagating radical of the polymer chain, located near the surfactant head group, captures monomer molecules or water phase radicals continuously diffusing from the water medium. If there are both monomer molecules and highly reactive small radical species present, the active site may preferentially be terminated by the small radicals. Therefore, we assume that the diffusing small species quickly terminate the radicals of living polymer chains without further propagation. Due to the rapid rate of termination, the termination rate constant K_t is a lumped parameter which accounts for the fact that $[R_w]$ and $[P_j^*]$ are actually concentrations in different phases (aqueous and particle, respectively). Thus, this lumps both the adsorption and termination steps.

$$[P_j^*] + [R_w] \xrightarrow{K_t} [P_j]$$

Model Formulation

The water phase radical species consist of primary radicals from initiator decomposition and desorbed monomeric radicals. The mass balance of the water phase radicals is:

$$\frac{d[R_w]}{dt} = 2fK_d[I_w] - K_2[R_w][N_t] - K_1[R_w][m_s] - K_h[R_w] + K_{de}[N_t][\bar{n}] - \frac{[R_w]}{\theta} \quad (2)$$

By using the stationary-state approximation, the above equation may be simplified to:

$$[R_w] = \frac{2fK_d[I_w] + K_{de}[N_t][\bar{n}]}{K_1[m_s] + K_2[N_t] + K_h} \quad (3)$$

where, $[I_w] \approx [I_F] \cdot (1 - e^{-t/\theta})$ for our start-up procedure, described in the Experimental Method section.

The monomeric radicals in the polymer particles are produced from absorption of water phase radicals into micelles and particles, and from transfer to monomer. These monomeric radicals are consumed by propagation, termination, and desorption. The mass balance on monomeric radicals in the particles is then:

$$\begin{aligned}\frac{d[P_o^*]}{dt} &= (\text{production of } [P_o^*]) - (\text{consumption of } [P_o^*]) \\ &= K_1[m_s]([R\cdot]_w + [M_1\cdot]) + K_2[N_o]([R\cdot]_w + [M_1\cdot]) \\ &\quad + K_{mf}\left[\sum_{j=1}^{\infty} P_j^*\right][M_p] - K_{de}[N_t][\bar{n}] - \left(K_p[M_p] + K_t[R_w] + K_{trp}\left[\sum_{j=1}^{\infty} P_j\right] + K_{pp}\left[\sum_{j=1}^{\infty} P_j\right] + \frac{1}{\theta}\right)[P_o^*] \\ &= K_1[m_s][R_w] + K_2[N_o][R_w] + K_{mf}\left[\sum_{j=1}^{\infty} P_j^*\right][M_p] - K_{de}[N_t][\bar{n}] - \left(K_p[M_p] + K_t[R_w] + K_{trp}\left[\sum_{j=1}^{\infty} P_j\right] + K_{pp}\left[\sum_{j=1}^{\infty} P_j\right] + \frac{1}{\theta}\right)[P_o^*] \end{aligned} \quad (4)$$

Using the quasisteady-state approximation and Eq. 3, the above equation is simplified to:

$$[P_o^*] = \frac{2fK_d[I_w] + K_{mf}\left[\sum_{j=1}^{\infty} P_j^*\right][M_p] - K_2[R_w][N^*] - K_h[R_w]}{K_p[M_p] + K_t[R_w] + K_{trp}\left[\sum_{j=1}^{\infty} P_j\right] + K_{pp}\left[\sum_{j=1}^{\infty} P_j\right] + \frac{1}{\theta}} \quad (5)$$

From the reaction steps, we can construct the set of differential equations for the living and dead polymer mass balances. The dead polymer mass balance is:

$$\frac{d[P_j]}{dt} = K_t[R_w][P_j^*] + K_{mf}[M_p][P_j^*] + K_{trp}[P_j^*]\left[\sum_{m=1}^{\infty} P_m\right] - K_{trp}[P_j]\left[\sum_{m=1}^{\infty} P_m^*\right] - K_{pp}[P_j]\left[\sum_{m=1}^{\infty} P_m^*\right] - \frac{[P_j]}{\theta} \quad (6)$$

The living polymer mass balance is:

$$\begin{aligned}\frac{d[P_j^*]}{dt} &= K_p[M_p][P_{j-1}^*] - K_p[M_p][P_j^*] - K_t[R_w][P_j^*] - K_{mf}[M_p][P_j^*] + K_{trp}[P_j]\left[\sum_{m=1}^{\infty} P_m^*\right] - K_{trp}[P_j^*]\left[\sum_{m=1}^{\infty} P_m\right] \\ &\quad + K_{pp}\left[\sum_{m=1}^{j-1} P_{j-m}^* P_m\right] - K_{pp}[P_j^*]\left[\sum_{m=1}^{\infty} P_m\right] - \frac{[P_j^*]}{\theta} \end{aligned} \quad (7)$$

From the infinite series of summations of Eq. 6 and Eq. 7 and the monomeric radical mass balance, a system of differential equations to calculate unsteady-state average molecular weights may be derived by using appropriate expressions for the moments and the series decomposition formula, which are both shown in Appendix A with detailed derivations for the series reduction.

The final set of differential equations obtained in terms of the moments is given in Eqs. 8 through 13. The variables A_i are defined in Appendix B.

$$\frac{d[M_o]}{dt} = (A_2)[M_o^*] - \left(A_3 + A_4 + \frac{1}{\theta}\right)[M_o] \quad (8)$$

$$\frac{d[M_1]}{dt} = (A_2)[M_1^*] - \left(A_3 + A_4 + \frac{1}{\theta}\right)[M_1] \quad (9)$$

$$\frac{d[M_2]}{dt} = (A_2)[M_2^*] - \left(A_3 + A_4 + \frac{1}{\theta}\right)[M_2] \quad (10)$$

$$\frac{d[M_o^*]}{dt} = (A_1)[P_o^*] - \left(A_2 + \frac{1}{\theta}\right)[M_o^*] + (A_3)[M_o] \quad (11)$$

$$\frac{d[M_1^*]}{dt} = (A_1)([P_o^*] + [M_o^*]) - \left(A_2 + \frac{1}{\theta}\right)[M_1^*] + (A_3 + A_4)[M_1] \quad (12)$$

$$\frac{d[M_2^*]}{dt} = (A_1)([P_o^*] + 2[M_1^*] + [M_o^*]) - \left(A_2 + \frac{1}{\theta}\right)[M_2^*] + (A_3 + A_4)[M_2] + 2K_{pp}[M_1^*][M_1] \quad (13)$$

where,

$$[P_o^*] = \frac{(A_6)}{\left(A_1 + A_5 + A_7 + \frac{1}{\theta}\right)}$$

By solving the above system of differential equations, weight and number average molecular weights can be calculated simply in terms of the zero, first, and second moments.

$$\overline{M_w} = (MW) \cdot \frac{([M_2] + [M_2^*])}{([M_1] + [M_1^*])} \quad (14)$$

$$\overline{M_n} = (MW) \cdot \frac{([M_1] + [M_1^*])}{([M_o] + [M_o^*])} \quad (15)$$

Careful observation of the above model tells us that the time-dependent variables of $[M_p]$ and $[N^*]$ are not determined within this model. To determine these variables, the model of Chiang and Thompson (1979) has been used. Thus, the molecular weight model developed here is used as a companion to Chiang and Thompson's model. All of the differential equations developed here together with Chiang and Thompson's model were solved numerically by using a Runge-Kutta algorithm on an IBM 3081 computer. All the solutions were obtained using less than 5 min CPU time.

Rate Parameter Values

One of the most important aspects in mathematical modeling is a suitable choice of rate parameter values. Table 1 presents parameter values determined by others and those used in this study. In this analysis, a set of parameter values was selected from among the available literature values to give the best results for conversion. This chosen parameter set was not optimized for particle size or molecular weight. As illustrated in Table 1, a wide range of rate parameter values has been reported in the literature for vinyl acetate polymerization at 60°C. These variations are due to somewhat different conditions of operation under which the rates are simply different. These values are also dependent on the model equations used. Table 2 presents our modified kinetic parameters for Chiang and Thompson's model (1979). All units are based on a unit volume of emulsion, following Kiparissides et al. (1979).

Experimental Method

Materials

Reagent grade vinyl acetate (VAc) supplied by Fisher Scientific Co. was further purified by distillation in a rotary evaporator at a reduced pressure of 30 mm Hg (4 kPa) to remove inhibitor. Sodium dodecyl sulfate (SDS) of 99% purity obtained from Sigma Chemical Co. was used without further purification. Initiator, potassium persulfate (PPS), from J.T. Baker Chemical Co. was used directly as obtained. Water was purified by reverse osmosis, then deionized and passed over a carbon filter before use. Nitrogen bubbled through a strongly akaline pyrogallol solution to remove trace oxygen was used to purge the reactor, as oxygen acts as a radical scavenger.

Reaction system

For continuous operation, two separate feed streams were prepared. One was the solution of vinyl acetate (1.333 L), SDS (9.6 g for a 0.01 mol/L water concentration) and distilled water (2.0 L). The other feed was the initiator solution (1.35 L water and 9.12 g PPS). To start up the reactor, the feed streams were introduced to a 1 L glass kettle reactor that was initially filled with 294 mL of distilled water. The two feed streams were continuously supplied to the stirred tank reactor at constant flow rates with a duplex-head masterflex pump (Cole-Parmer Co.) through silicone tubing. Flow rates were 7 mL/min for monomer solution and 2.8 mL/min for initiator solution. The reactor temperature was maintained at 60° ±2°C. The conversion of the effluent emulsion was measured continuously by a Mettler Paar DMA 35 densitometer. Samples of the effluent emulsion were quenched by concentrated hydroquinone solution, and were stored in 10 mL sampling bottles. Samples were taken every 10 min for analysis of molecular weights and particle size. Particle size was measured immediately, while molecular weights were determined after coagulation and drying of the samples. The basic design follows that of Kiparissides et al. (1979, 1980a,b).

Average particle sizes were estimated by quasi-elastic light scattering on a Coulter model N4-SD laser light scattering system using their onboard size distribution processor. Molecular weight distributions of the polymer were determined by gel per-

Table 1. Variations in Major Kinetic Parameters at 60°C

Parameters	Friis et al. (1974)	Chiang & Thompson (1979) (40°C)	Baade et al. (1982)	Villermaux et al. (1983)	Taylor & Reichert (1985)	This Study
K_p	3,910	4,068	9,500	11,900	9,500	9,500
K_{mf}	1.19	0.75	2.26	2.56	2.34	1.20
K_{pp}	*	—	6,270	2,689	6,270	*
K_{trp}	1.88	—	3.23	3.61	0.49	1.88
$K_t(\times 10^{-8})$	—	—	3.55	0.73	3.55	0.73

Units are L/mol · s

*Parameter varies with conversion:

$$X \le 0.21, \quad K_{pp} = 2{,}213.4$$

$$X > 0.21, \quad K_{pp} = 2{,}213.4 - 169.6X - 479X^2 - 1{,}014X^3$$

Table 2. Kinetic Parameters for Chiang and Thompson's Model

Parameters	Values
D_w	10^{-7} dm^2/s
δ	0.55
f	0.6
K_d	0.0015 1/h
K_1	9.85×10^{-13} cm^3/no. · h
K_2	$5K_1 \times (d_p/d_m)^2$ cm^3/no. · h
L	1.3×10^{-4} dm
S_α	6.10×10^{-17} dm^2/molec.
K_{ho}	0.172 1/h, $K_h = K_{ho} \cdot [1 - (A_p/4)L]$
K_{de}	*
D_p	1.4×10^{-9} dm^2/s, for high conversion

*Parameter varies with conversion:

$$\text{For low conversion, } K_{de} = \left[\frac{12D_w\delta}{md_p^2}\right] \cdot \left[\frac{K_{mf}}{K_p}\right]$$

$$\text{For high conversion, } K_{de} = \left[\frac{6D_p}{d_p^2}\right] \cdot \left[\frac{K_{mf}}{K_p}\right]$$

meation chromatography using a Waters Associates model GPC 1 apparatus with a differential refractometer and three 7.8 mm × 30 cm columns packed with ultra-styragel having nominal pore sizes of 1×10^3, 1×10^5, and 1×10^6 Å. Tetrahydrofuran was used for the solvent.

Results and Discussion

Conversion and average particle size

In the model development, all of the phenomena thought to be of significance in the emulsion polymerization of vinyl acetate have been included. Figure 1 shows the results of our implementation of Chiang and Thompson's differential equations for conversion using the parameter values that have been discussed. The simulations at 60°C for three surfactant concentrations are compared with our experimental results. The model underestimates the experimental conversion slightly at an SDS concentration of 0.05 mol/L water, but the predictions at the two lower surfactant concentrations agree very well with the data.

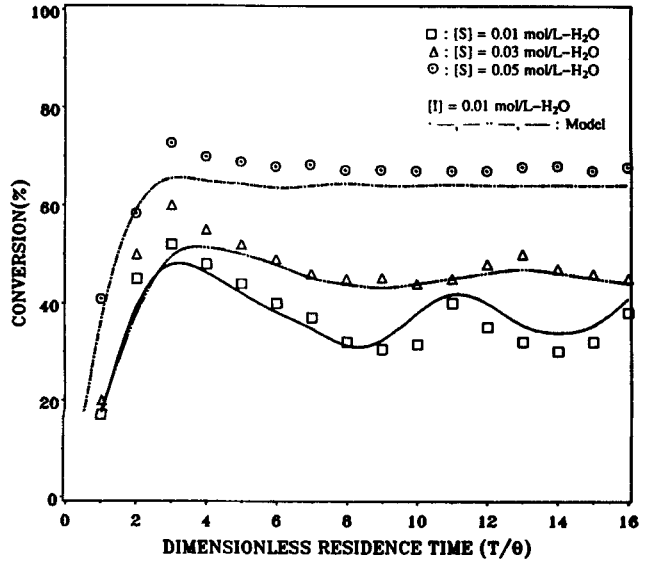

Figure 1. Conversion vs. dimensionless time at 60°C.
θ = 30 min.; VAc/water = 4/10

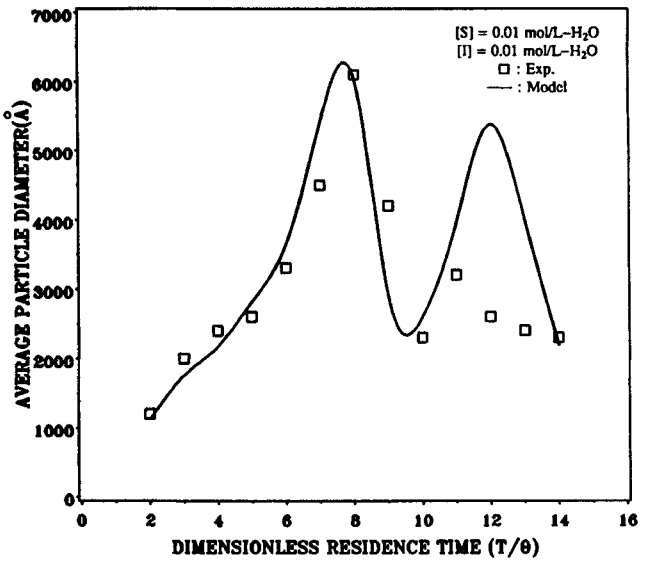

Figure 2. Average particle size vs. dimensionless time at 60°C.
θ = 30 min.; VAc/water = 4/10

In Figures 2 through 4, the comparison between our experimental results for particle size and the simulations of Chiang and Thompson's model is made. At the lowest surfactant concentration, the results shown in Figure 2, the agreement is reasonable, although the reduction in the particle size at the second maximum, occurring at t/θ of 10.5 is considerably less for the model results compared with that observed experimentally. Figure 3 shows that the agreement at higher surfactant concentration is poor, with the experimental results showing considerably less sensitivity than the simulation. At even higher surfactant concentration, a fivefold increase over that of Figure 2, the

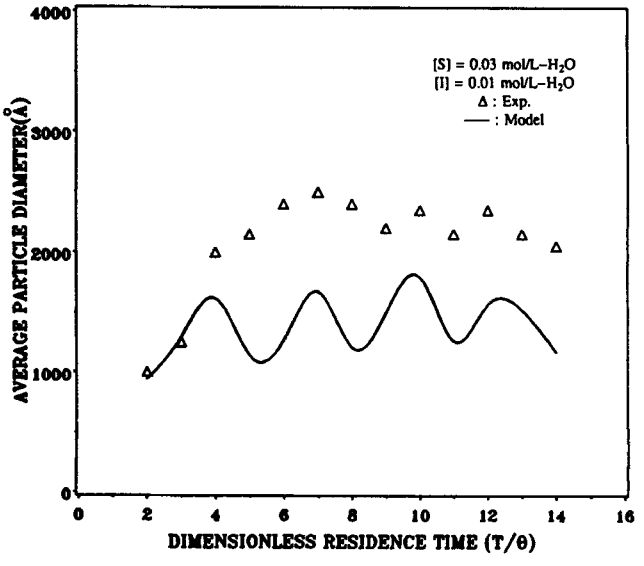

Figure 3. Average particle size vs. dimensionless time at 60°C.
θ = 30 min.; VAc/water = 4/10

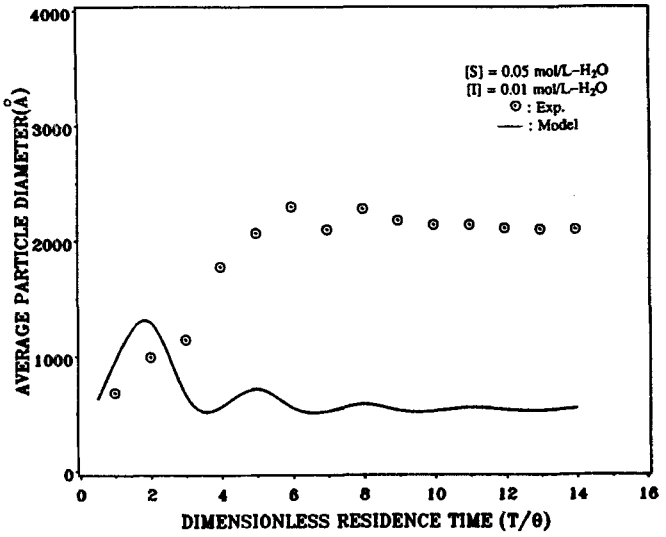

Figure 4. Average particle size vs. dimensionless time at 60°C.

θ = 30 min., VAc/water = 4/10

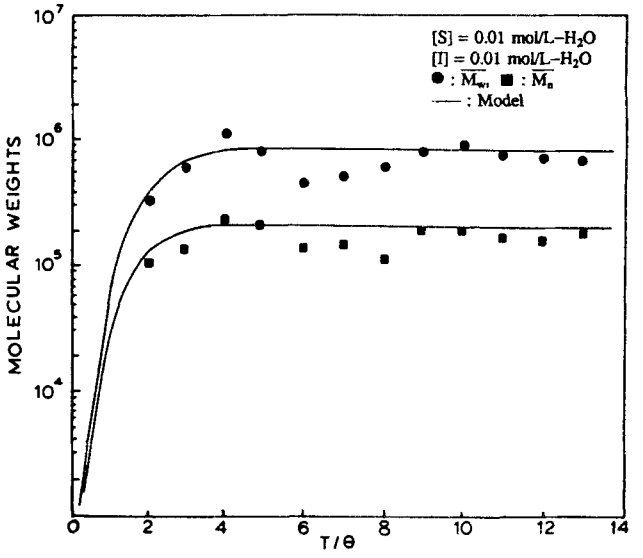

Figure 5. Molecular weight vs. dimensionless time at 60°C.

θ = 30 min.; VAc/water = 4/10

results continue the trend as shown in Figure 4. While the damping of the oscillations is observed both experimentally and in the prediction, clearly the model results severely underestimate the observed particle size. Adjustment of D_w and ϵ can improve the results to some extent, but the average particle size calculated remains substantially too small. Edelhauser (1969) suggested that sodium dodecyl sulfate, which has a relatively short carbon chain length, tends to penetrate into the interior of polyvinyl acetate particles, causing swelling and gradual dissolution of polymer chains by generating solubilized polymeric complexes in the manner of a polyelectrolyte. However, this disintegration of polymer chains leads only to limited swelling of the particles. The reason for this is that formation of a polyvinyl alcohol (protective colloid) layer by hydrolysis of polyvinyl acetate around the particle inhibits the swelling (El-Aasser and Vanderhoff, 1981). This interaction phenomenon between surfactant and polymer chains is not considered in the theoretical model. Also, in some cases laser light scattering is known to undercount or ignore particles in the smallest ranges, and this could be a contributing cause to this discrepancy in results. However, the fact that the average particle size from the experiments agrees fairly well at low surfactant concentrations (evidently not ignoring smaller particles) and shows no sensitivity to the surfactant concentration in this range, might imply that the model's sensitivity to this variation is too large. This model has been shown to provide satisfactory results for modeling transient continuous stirred tank emulsion polymerization behavior of conversion (Kiparissides et al., 1979; Chiang and Thompson, 1979), and it is difficult to estimate the effects of the uncertainty of parameter values in such a complex model without extensive efforts in that direction.

Molecular weight

Figure 5 shows the results of the experiments and simulation for this system at a surfactant concentration of 0.01 mol/L water. The observed weight average molecular weight and polydispersity ratio are around 0.78×10^6 and 4.3, respectively. When maximum average particle sizes are observed at the dimensionless residence times of 6 and 8 in Figure 2, approximately minimum average molecular weights are observed. From a kinetic point of view, smaller particle sizes and higher particle numbers give higher molecular weights due to longer propagation times. It can be seen that the model results agree very well with the experimental data for both weight average and number average molecular weights. The model results, however, do not show the oscillations that are present in the experimental results. In fact the model results do oscillate, but only with very low amplitudes that cannot be observed on the scales of the figures shown here. In Figures 6 and 7, where the surfactant concentrations are 0.03 and 0.05 mol/L water, respectively, the same behavior is observed. The weight average molecular weights are 0.9×10^6 and 1.2×10^6, and the observed polydispersity ratios are approximately 4.4 and 7.8. For the surfactant concentration of 0.05 mol/L water, the desorption rate expression for high conversion range shown in Table 2 was used for the prediction. For both weight average molecular weights, the theoretical results approximate the general trends very well. However, for number average molecular weights at surfactant concentration of 0.05 mol/L water, the model results do not agree with the experimental results. A modified formula that corresponds to the Smith-Ewart second idealized mechanism, which is known to give higher polydispersity ratios, was tried, but the prediction was not satisfactory. As the surfactant concentration increases, the model generally tends to be more sensitive to molecular weight than the experimental results. Theoretically, higher surfactant concentrations result in smaller average particle sizes, and smaller particle sizes give higher molecular weights. This discrepancy may be explained by the interaction between surfactant and polymer chains, as mentioned previously. The use of higher surfactant concentrations may promote the chain disintegration and solubilization. As a result, propagating polymer chains may be terminated at lower degrees of polymerization and thus larger polydispersities occur. However, there is no conclusive evidence for this explanation.

The goal of this work has been to develop a model that repre-

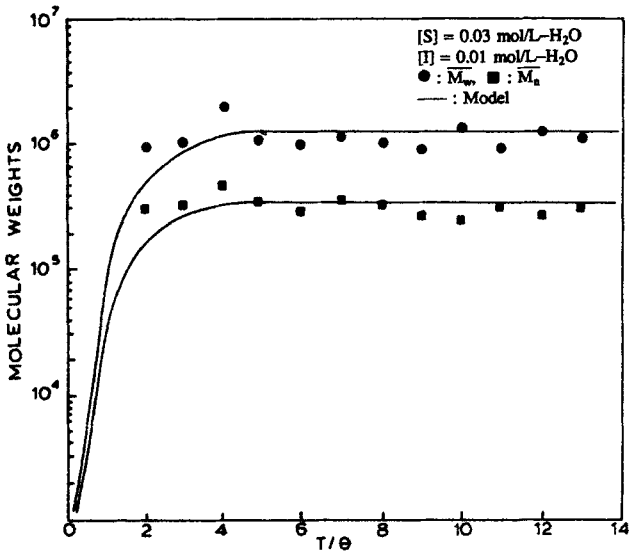

Figure 6. Molecular weight vs. dimensionless time at 60°C.
θ = 30 min.; VAc/water = 4/10

sents the number and weight average molecular weights and the polydispersity during the polymerization. In this model, all of the major phenomena associated with the kinetics involving control of chain length of the polymer have been included. Through the simulations using this molecular weight model, it has been found that the oscillations of molecular weight and polydispersity are closely related to alteration of the initiation mechanism, which results in variations of the monomeric radical concentration in the particles. When this monomeric radical concentration approaches a constant value, the simulated result of molecular weight converges to a constant value, i.e., weight and number average molecular weights do not oscillate. When the monomeric radical concentration is zero, the limiting polydispersity ratio is 2.2. This implies that if the initiation mechanism is neglected, the predicted result would have a polydispersity ratio of 2.2, which is the theoretical result obtained in a segregated reactor model (Lichti et al., 1980).

Although the values of the propagation and transfer rate constants have strong effects on the amount of high molecular weight polymer generated, they do not significantly affect the polydispersity oscillations. In contrast, it was found that adjustment of the value of the radical desorption rate constant could produce oscillations in the molecular weights of the magnitude seen experimentally. Therefore, it is believed that the main reason that the model does not generate the appropriate oscillations at low surfactant concentrations is the inaccurate estimation of the radical desorption rate constant. In addition, the monomeric radical mass balance used in this study may be oversimplified. Generally the monomeric radical concentration is very small and small variations in its value create large deviations in the molecular weights and polydispersities. Equation 5 shows that the monomeric radical concentration is highly dependent on the absorption and desorption rates. Actually, this small species concentration alone does not affect the global average molecular weight. Variations, or higher values, of the monomeric radical concentration correspond directly to the same behavior of the total propagating radical concentration in polymer particles. Therefore, this concentration is a good indicator representing the total radical concentration change in the particles. Clearly, the oscillations of molecular weight and polydispersity are due to variations of the total radical concentration in the particles. In the model simulation, to predict the radical absorption and desorption rates, the experimental data and approximate models of Nomura and Harada (1981) and Nomura (1982) were used. Figure 8 shows that adjustment of the desorption rate constant gives a good approximation for the period and magnitude of the observed oscillations. In Figure 8, the desorption rate constant was reduced to one-tenth of the original value by adjusting the

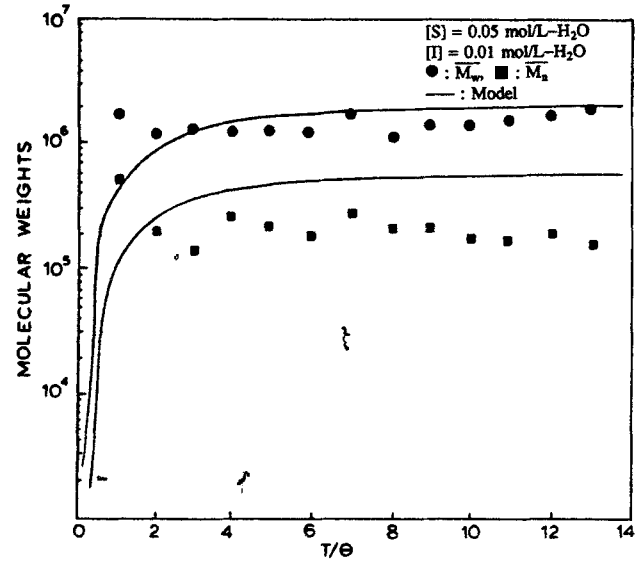

Figure 7. Molecular weight vs. dimensionless time at 60°C.
θ = 30 min.; VAc/water = 4/10; K_{de} for high conversion range used

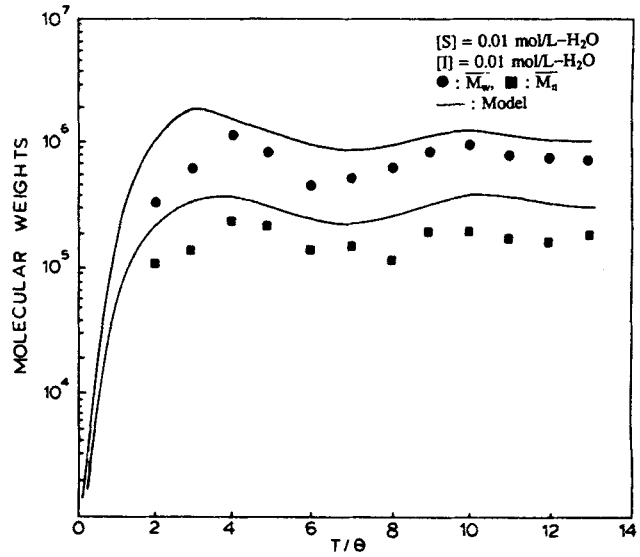

Figure 8. Molecular weight vs. dimensionless time at 60°C.
θ = 30 min.; VAc/water = 4/10; K_{de} reduced to about 0.1 original value

values of D_w. Through model simulation, in which the desorption rate constant was varied, it was concluded that an appropriate desorption rate constant value significantly improves the prediction by causing oscillations to occur, although variation of this one parameter also causes an overshoot of the average values. Therefore, the success of the molecular weight prediction appears to be very sensitive to the radical desorption rate during the polymerization. Chern and Poehlein (1987) developed an alternative expression for the radical desorption rate constant by taking into consideration the nonuniform distribution of monomeric radicals in the particles. This new equation suggests a larger value for the desorption rate constant. However, it appears that a lower value for the desorption rate constant is more appropriate in this molecular weight simulation. In order to achieve results where both the oscillations and good average values of these variables are obtained, a systematic sensitivity analysis would be advantageous to determine the most appropriate manipulation of parameter values.

Conclusions

A detailed mathematical model to predict molecular weight variations in continuous stirred tank vinyl acetate polymerization has been developed by using a moment method. Special consideration has been given to initiation and termination mechanisms. The molecular weight oscillations, which are often observed in continuous emulsion polymerization, are associated with a heterogeneous initiation mechanism that involves radical desorption and absorption phenomena. It is found that the effective radical diffusion coefficient in the water phase is a key parameter in causing the molecular weight oscillations.

Generally, the model predicts the correct trends of experimental data for the average molecular weights. However, it fails to adequately account for the magnitude of the oscillations when existing values of the important rate parameters from the literature are used. The model does show the capability of modeling these oscillations when the parameters are adjusted. Actual tuning of the appropriate parameters would optimally be accomplished by sensitivity studies.

Acknowledgment

We wish to acknowledge partial support of this work by the University of Oklahoma Associates Fund and by Coulter Electronics.

Notation

d_m = micelle diameter
d_p = particle diameter
D_p = self-diffusion constant of a monomeric radical in particles
D_w = effective radical diffusion coefficient in water phase
f = initiator efficiency factor
$[I_F]$ = initiator concentration in feed
K_1 = radical absorption rate constant to micelles
K_2 = radical absorption rate constant to particles
K_d = initiator decomposition rate
K_{de} = radical desorption rate constant
K_h = homogeneous nucleation constant
K_i = initiation rate constant
K_{mf} = radical transfer rate constant to monomer
K_p = radical propagation rate constant
K_{pp} = terminal double bond reaction constant
K_{trp} = radical transfer constant to polymer
K_t = termination rate constant
L = radical diffusion length in water phase
m = radical partition coefficient between water phase particles
m_s = micelle concentration
$[M_o]$ = zero moment for dead polymer
$[M_1]$ = first moment for dead polymer
$[M_2]$ = second moment for dead polymer
$[M_o^*]$ = zero moment for living polymer
$[M_1^*]$ = first moment for living polymer
$[M_2^*]$ = second moment for living polymer
$\overline{M}_w$ = weight average molecular weight
$\overline{M}_n$ = number average molecular weight
$[M_p]$ = monomer concentration in particles
$[M_1\cdot]$ = monomeric radical concentration in water phase
(MW) = vinyl acetate molecular weight
$[N_o]$ = dead particle concentration
$[N_t]$ = total particle concentration
$[N^*]$ = active particle concentration
$[\bar{n}]$ = average number of radicals per particle
$[P_j^*]$ = living polymer concentration in particles
$[P_j]$ = dead polymer concentration
$[P_o^*]$ = monomeric radical concentration in particles
$[R_w]$ = water phase radical concentration (primary radical concentration + monomeric radical concentration)
$[R\cdot]_w$ = primary radical concentration in water phase
$[R\cdot]_p$ = absorbed primary radical concentration in micelles and polymer particles
S_α = area covered by one molecule of SDS
t = time
X = conversion

Greek letters

δ = lumped monomeric radical diffusion coefficient
ϵ = ratio of radical absorption rates

Appendix A: Moment Expressions and Series Reductions

$$[M_i] = \left[\sum_{j=1}^{\infty} j^i \cdot P_j\right], \text{ for dead polymer}$$

$$[M_i^*] = \left[\sum_{j=1}^{\infty} j^i \cdot P_j^*\right], \text{ for living polymer}$$

$$\left[\sum_{j=1}^{\infty} P_{j-1}^*\right] - \left[\sum_{j=1}^{\infty} P_j^*\right] = [P_o^*] - [P_\infty^*] = [P_o^*]$$

$$\left[\sum_{j=1}^{\infty}\sum_{m=1}^{j-1} P_{j-m}^* P_m\right] = \left[\sum_{j=1}^{\infty} P_j^*\right]\left[\sum_{j=1}^{\infty} P_j\right] = [M_o^*][M_o]$$

$$\left[\sum_{j=1}^{\infty} j \cdot P_{j-1}^*\right] - \left[\sum_{j=1}^{\infty} j \cdot P_j^*\right] = [P_o^*] + [M_o^*]$$

$$\left[\sum_{j=1}^{\infty}\left(j \cdot \sum_{m=1}^{j-1} P_{j-m}^* P_m\right)\right] = [M_1^*][M_o] + [M_o^*][M_1]$$

$$\left[\sum_{j=1}^{\infty} j^2 \cdot P_{j-1}^*\right] - \left[\sum_{j=1}^{\infty} j^2 \cdot P_j^2\right] = [P_o^*] + 2 \cdot [M_1^*] + [M_o^*]$$

$$\left[\sum_{j=1}^{\infty}\left(j^2 \cdot \sum_{m=1}^{j-1} P_{j-m}^* P_m\right)\right] = [M_2^*][M_o] + 2 \cdot [M_1^*][M_1] + [M_o^*][M_2]$$

Appendix B: Simplified Notation

$$A_1 = K_p[M_p]$$

$$A_2 = K_t[R_w] + K_{mf}[M_p] + K_{trp}\left[\sum_{j=1}^{\infty} P_j\right]$$

$$A_3 = K_{trp}\left[\sum_{j=1}^{\infty} P_j^*\right]$$

$$A_4 = K_{pp}\left[\sum_{j=1}^{\infty} P_j^*\right]$$

$$A_5 = K_{pp}\left[\sum_{j=1}^{\infty} P_j\right]$$

$$A_6 = 2fK_d[I_w] + K_{mf}\left[\sum_{j=1}^{\infty} P_j^*\right][M_p] - K_2[N^*][R_w] - K_h[R_w]$$

$$A_7 = K_t[R_w] + K_{trp}\left[\sum_{j=1}^{\infty} P_j\right]$$

Literature Cited

Baade, W., H. U. Moritz, and K. H. Reichert, "Kinetics of High Conversion Polymerization of Vinyl Acetate. Effects of Mixing and Reactor Type on Polymer Properties," *J. Appl. Polym. Sci.*, **27**, 2249 (1982).

Chern, C., and G. W. Poehlein, "Polymerization in Nonuniform Latex Particles: Distribution of Free Radicals," *J. Polym. Sci.: Polym. Chem.*, **25**, 617 (1987).

Chiang, A. T., and R. W. Thompson, "Modeling the Transient Behavior of Continuous Emulsion Polymer Reactors," *AIChE J.*, **25**, 552 (1979).

Dickinson, R. F., "Dynamic Behaviour and Minimum Norm Control of Continuous Polymerization Chains," Ph.D Thesis, Univ. Waterloo, Ont. Canada (1976).

Edelhauser, H. A., "Investigation of the Disposition of Surfactant in a Latex by the Rate of Dialysis Method. Mechanism of Detergent Dialysis" *J. Polym. Sci. Part C*, **27**, 291 (1969).

El-Aasser, M. S., and J. W. Vanderhoff, *Emulsion Polymerization of Vinyl Acetate*, Applied Science Pub., NJ (1981).

Friis, N., and A. E. Hamielec, "Kinetics of Vinyl Chloride and Vinyl Acetate Emulsion Polymerization," *J. Appl. Polym. Sci.*, **19**, 97 (1975).

Friis, N., D. Goosney, J. D. Wright, and A. E. Hamielec, "Molecular Weight and Branching Development in Vinyl Acetate Emulsion Polymerization," *J. Appl. Polym. Sci.*, **18**, 1247 (1974).

Graessley, W. W., R. D. Hartung, and W. C. Uy, "Studies of Branching in Polyvinyl Acetate," *J. Polym. Sci. Part A-2*, **7**, 1919 (1969).

Greene, R. K., R. A. Gonzalez, and G. W. Poehlein, "Continuous Emulsion Polymerization—Steady State and Transient Experiments with Vinyl Acetate and Methyl Methacrylate," *Emulsion Polymerization*, I. Piirma, J. L. Gardon, eds., *Am. Chem. Soc. Symp. Ser.*, **24**, 341 (1976).

Hansen, F. K., and J. Ugelstad, "Particle Nucleation in Emulsion Polymerization. I: A Theory for Homogeneous Nucleation," *J. Polym. Sci.*, **16**, 1953 (1978).

———, "Particle Nucleation in Emulsion Polymerization. II: Nucleation in Emulsifier-Free System Investigated by Seed Polymerization" *J. Polym. Sci.*, **17**, 3033 (1979).

Harkins, W. D., "A General Theory of the Reaction Loci in Emulsion Polymerization" *J. Chem. Phys.*, **13**, 381 (1945).

———, "A General Theory of the Reaction Loci in Emulsion Polymerization. II," *J. Chem. Phys.*, **14**, 47 (1946).

———, "A General Theory of Mechanism of Emulsion Polymerization," *J. Am. Chem. Soc.*, **69**, 1428 (1947).

Kirillov, V. A., and W. H. Ray, "The Mathematical Modeling of Continuous Emulsion Polymerization Rector," *Chem. Eng. Sci.*, **33**, 1499 (1978).

Kiparissides, C., "Modelling and Experimental Studies of a Continuous Emulsion Polymerization Reactor," Ph.D. Thesis, McMaster University, Hamilton, Ontario (1978).

Kiparissides, C., J. F. MacGregor, and A. E. Hamielec, "Continuous Emulsion Polymerization: Modelling Oscillations in Vinyl Acetate Polymerization," *J. Appl. Polym. Sci.*, **23**, 401 (1979).

———, "Continuous Emulsion Polymerization of Vinyl Acetate. I: Experimental Studies," *Can. J. Chem. Eng.*, **58**, 48 (1980a).

———, "Continuous Emulsion Polymerization of Vinyl Acetate. II: Parameter Estimation and Simulation Studies," *Can. J. Chem. Eng.*, **58**, 56 (1980b).

Lichti, G., R. G. Gilbert, and D. H. Napper, "Molecular Weight Distributions in Emulsion Polymerizations," *J. Polym. Sci. Polym. Chem. Ed.*, **18**, 1297 (1980).

Min, K. W., and W. H. Ray, "On Mathematical Modeling of Emulsion Polymerization Reactors," *J. Macro. Sci. Revs.*, **C11**, 177 (1974).

Nagasubramanian, K., and W. W. Graessley, "Continuous Reactors in Free Radical Polymerization with Branching. I: Theoretical Aspects and Preliminary Considerations" *J. Chem. Eng. Sci.*, **25**, 1549 (1970).

Nomura, M., "Desorption and Reabsorption of Free Radicals in Emulsion Polymerization," *Emulsion Polymerization*, I. Pirma, ed., Academic Press, New York, 191 (1982).

Nomura, M., and M. Harada, "Rate Coefficient for Radical Desorption in Emulsion Polymerization," *J. Appl. Polym. Sci.*, **26**, 17 (1981).

Omi, S., T. Ueda, and H. Kubota, "Continuous Operation of Emulsion Polymerization of Styrene," *J. Chem. Eng. Japan*, **2**, 193 (1969).

O'Toole, J. T., "Kinetics of Emulsion Polymerization," *J. Appl. Polym. Sci.*, **9**, 129 (1965).

Pollock, M., J. F. MacGregor, and A. E. Hamielec, "Continuous Polyvinyl Acetate Emulsion Polymerization Reactors: Dynamic Modeling of Molecular Weight and Particle Size Development and Application to Optimal Multiple Reactor System Design," *Computer Applications in Applied Polymer Science*, T. Provder, ed., *Am. Chem. Soc. Symp. Ser.*, **197**, 209 (1982).

Rawlings, J. B., "Simulation and Stability of Continuous Emulsion Polymerization Reactors," Ph.D Thesis, Univ. Wisconsin, Madison (1985)

Rawlings, J. B., and W. H. Ray, "Emulsion Polymerization Reactor Stability: Simplified Model Analysis," *AIChE J.*, **33**, 1663 (1987).

Rosen, M. J., *Surfactants and Interfacial Phenomena*, Wiley, New York (1978).

Saito, O., K. Nagasubramanian, and W. W. Graessley, "Molecular Weight Distribution in Branched Polymers," *J. Polym. Sci. Part A-2*, **7**, 1937 (1969).

Smith, W. V., and R. H. Ewart, "Kinetics of Emulsion Polymerization," *J. Chem. Phys.*, **16**, 592 (1948).

Stockmayer, W. H., "Notes on the Kinetics of Emulsion Polymerization," *J. Polym. Sci.*, **24**, 314 (1957).

Taylor, T. W., and K. H. Reichert, "The Influence of Reactor Type and Operating Conditions on the Molecular Weight Distribution in Vinyl Acetate Polymerization," *J. Appl. Polym. Sci.*, **30**, 227 (1985).

Ugelstad, J., and F. K. Hansen, "Kinetics and Mechanism of Emulsion Polymerization," *Rubber Chem. Tech.*, **49**, 536 (1976).

Villemaux, J., L. Blavier, and M. Pons, *Polymer Reaction Engineering*, K. H. Reichert, W. Geiseler, eds., Hanser, Munich (1983).

Manuscript received Apr. 26, 1987, and revision received Jan 15, 1988.